Orthogonal amplification circuits composed of acyclic nucleic acids enable RNA detection

Yanglingzhi Chen, Ryuya Nagao, Keiji Murayama*, and Hiroyuki Asanuma*

Graduate School of Engineering, Nagoya University, Furo-cho, Chikusa-ku, Nagoya 464-8603, Japan.

ABSTRACT: Construction of complex DNA circuits is difficult due to unintended hybridization and degradation by enzymes under biological conditions. We herein report hybridization chain reaction (HCR) circuit composed of left-handed *acyclic* D-threoninol nucleic acid (D-*a*TNA), which is orthogonal to right-handed DNA and RNA. Because of its high thermal stability, use of an *a*TNA hairpin with a short 7 base-pair stem ensured clear ON-OFF control of the HCR circuit. The *a*TNA circuit was stable against nucleases. A circuit based on right-handed *acyclic* L-threoninol nucleic acid (L-*a*TNA) was also designed, and high orthogonality between D- and L-*a*TNA HCRs was confirmed by activation of each *a*TNA HCR via a corresponding input strand. A dual OR logic gate was successfully established using serinol nucleic acid (SNA), which could initiate both D- and L-*a*TNA circuits. The D-*a*TNA HCR was used for RNA-dependent signal amplification system via the SNA-interface. The design resulted in 80% yield of the cascade reaction in 3000 s without significant leak. This work represents the first example of use of heterochiral HCR circuits for detection of RNA molecules. The method has potential for direct visualization of RNA *in vivo* and FISH method.

INTRODUCTION

DNA circuits that rely on toehold-mediated strand displacement[1] have been used for digital circuit computation,[2-5] biomolecular sensing,[6-9] nanomachines,[10-13] alignment of molecules,[14-16] and functional macromaterials.[17,18] These circuits are achieved via an orthogonality based on DNA sequence complementarity. However, some mismatched base pairs are tolerated in long sequences and partially complementary sequences can interact with each other to form unintended duplexes, triplexes, quadruplexes, and other higher ordered structures, which inhibit circuit function.

Use of orthogonal artificial nucleic acids could potentially enhance circuit accuracy and efficiency. Artificial nucleic acids with modifications on the mainchain scaffold, referred to as xeno-nucleic acids (XNAs), have been widely studied.[19-23] Several orthogonal XNAs that cannot hybridize to DNA and RNA, but form homo-duplex have also been reported.[24-29] Induction of inversed helicity is an effective approach to facilitate the orthogonality. For example, right-handed D-DNA and left-handed L-DNA do not cross-hybridize with each other even though sequences are complementary.[30-35] Sczepanski *et al.* designed a heterochiral nucleic acid circuit using combination of D-DNA, L-DNA, and achiral PNA.[36] Ly *et al.* reported γ-peptide nucleic acid (γPNA); its helicity is controlled by a chiral center at the γ-position on the backbone.[37,38] Right-handed γPNA cross-hybridizes with D-DNA and D-RNA, whereas left-handed γPNA does not. Such helical orthogonality holds promises for parallel processing of a DNA circuit and an orthogonal XNA circuit.[39]

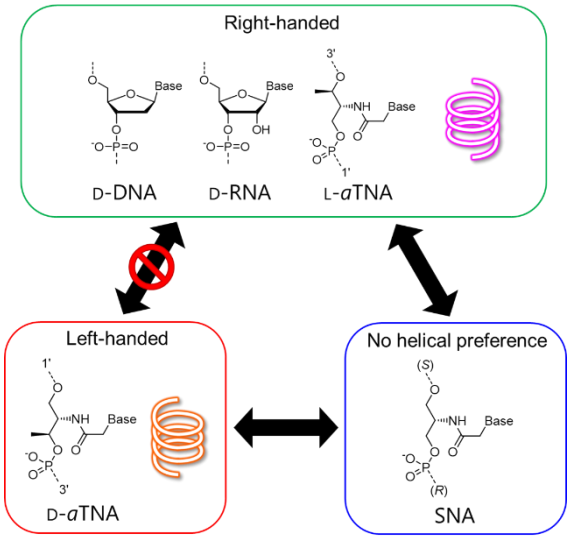

Figure 1. Chemical structures, helicities, and hybridization compatibilities of DNA, RNA, D-*a*TNA, SNA, and L-*a*TNA. Oligonucleotides belonging to the right-handed group can form homo- and hetero-duplexes with each other, whereas D-*a*TNA with left-hand helicity cannot hybridize with oligonucleotides from the right-handed group. SNA has a symmetrical scaffold and can hybridize with both oligonucleotides belonging to right- and left-handed helicity groups.

Our group has developed three kinds of *acyclic* XNAs; *acyclic* D-threoninol nucleic acid (D-*a*TNA),[27] serinol nucleic acid (SNA),[40] and *acyclic* L-threoninol nucleic acid (L-*a*TNA).[41] Left-handed D-*a*TNA is orthogonal to right-handed D-DNA, D-RNA and L-*a*TNA, whereas SNA, which has a symmetric linker with no helical preference, can hybridize with oligonucleotides irrespective of their helicities (Figure 1).[40] The non-helical SNA can serve as an interface between the left-handed and right-handed oligonucleotides.[42] Herein, we demonstrate a

hybridization chain reaction (HCR) in which an input strand triggers sequential opening of two hairpin strands to generate a long duplex. This strategy is applicable in variety of functional tools.[6,14,16,17,43-49] We also demonstrated an orthogonal HCR circuit composed of left-handed D-*a*TNA and right-handed L-*a*TNA with same sequences, which can be activated specifically by *a*TNAs with desired chirality. These orthogonal circuits were also utilized in an OR gate by combination with SNA, which can interact with both circuits. Finally, a D-RNA-triggered D-*a*TNA HCR mediated by an SNA interface was established. This design would be used for RNA detection *in vivo* and for biopsy samples.

RESULTS AND DISCUSSION

Characterization of D-*a*TNA HCR. We first designed a D-*a*TNA HCR with a 13-mer input (DT-Input) and DT-HP1 and DT-HP2 hairpins with 6-mer toehold/loop and 7-base pair (bp) stem (Figure 2a). DT-HP2 tethers Cy3 as a fluorophore and Nitro methyl red as a quencher at 1' and 3' termini of stem region, respectively (Figure S1). This system enables observation of the elongation reaction by fluorescence emission of Cy3. The melting temperature (T_m) of the stem of DT-HP2 was over 80 °C (Figure S2), indicating that the stem was sufficiently stable despite the short sequences.

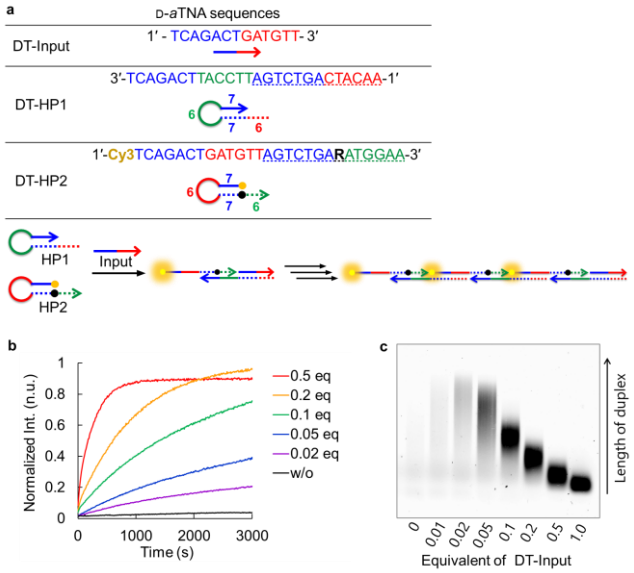

Figure 2. (a) Sequence design and schematic illustration of D-*a*TNA HCR circuit. (b) Time trace of signal generated from D-*a*TNA HCR triggered by DT-Input with indicated equivalents of each hairpin. Conditions: 37 °C, 10 mM phosphate buffer, 100 mM NaCl, pH 7.0, 100 nM DT-HP1, 100 nM DT-HP2. Fluorescence intensity was normalized by the maximum emission of the *a*TNA HCR trigger by 20 nM DT-Input. (c) Agarose gel analysis (2 w/v%) of the D-*a*TNA HCR product after 2 h with indicated amount of DT-Input.

The reaction was conducted in phosphate buffer with 100 mM NaCl. Upon the addition of DT-Input into the solution containing DT-HP1 and DT-HP2, signal amplification was observed, whereas almost no emission was attained in the absence of the DT-Input (Figure 2b). The amplification kinetics depended on the concentration of DT-Input: A higher amounts of DT-Input results in a faster reaction rate. For example, 3000 s after the addition of the 0.2 eq. DT-Input, about 95% hairpin was opened based on the fluorescence signal (Figure 2b). The reaction by 0.05 eq. DT-Input resulted in slower kinetics, and the fluorescent intensity finally reached equilibrium, probably because the possible product length has a limitation (Figure S3). Lengths of HCR products were characterized using agarose gel electrophoresis (Figure 2c). Long products with high dispersity were formed in the reaction at lower concentrations of DT-Input. In the absence of DT-Input, no band was observed. Lengths of *a*TNA HCR product were about 100-500 bp, corresponding to 8-40 hairpins, which are similar to the canonical DNA-HCR products (Figure S4).[6] Nuclease resistance of D-*a*TNA HCR circuit was evaluated in 10% fetal bovine serum (FBS). Since the D-*a*TNA scaffold could not be recognized by nuclease, the D-*a*TNA HCR circuit operated even in the 10% FBS, whereas a circuit with a DNA hairpin exhibited only nonspecific emission in the presence of the FBS (Figure S5). Generally, DNA-HCR requires hairpins with at least 12-bp stem to inhibit leak reactions, and sequence design is complicated.[6,50] In contrast, the circuit composed of the D-*a*TNA hairpin with a 7-bp stem had low background emission, rapid elongation, and high durability against nucleases, comparable with PNA-based HCR composed of short hairpins (5-bp), recently reported by Winssinger et al.[51] Compared to PNA, *a*TNAs have the advantages of high solubility due to the negatively charged backbones and facile synthesis via conventional phosphoramidite method using DNA synthesizer, which enables synthesis of a wide range of sequences, like DNA.

Orthogonal HCR. Next, we synthesized an L-*a*TNA HCR circuit designed to be orthogonal to the D-*a*TNA HCR circuit. The same sequences used for the D-*a*TNA HCR were used except that Cy5 was used as the fluorophore (Figure 3a, Figure S1). Here we used phosphate buffer containing 200 mM NaCl to improve the response. The signal from the L-*a*TNA HCR circuit was amplified quickly and reached equilibrium within the 1200 s after the addition of 0.2 eq. LT-Input (Figure 3b). There was more leakage from the L-*a*TNA HCR circuit than from the D-*a*TNA HCR circuit. Since the same sequences were used between D-*a*TNA HCR and L-*a*TNA HCR, large leakage was probably due to the steric hindrance from the larger Cy5 and flexible propane linker between Cy5 and the strand, which possibly enhance breezing effect that induces unspecific open of HP2. Since D-*a*TNA is orthogonal to L-*a*TNA, DT-Input, which has same sequence with LT-Input, did not activate the L-*a*TNA HCR circuit (Figure 3c). Similarly, D-*a*TNA HCR was not initiated by LT-Input (Figure 3d, e). Thus, opposite helicities of D- and L-*a*TNA allowed us to establish an orthogonal HCR system.

SNA interacts with both L- and D-*a*TNAs because SNA has no helical preference due to its achiral scaffold. An SNA input strand (S-Input) activated both D- and L-*a*TNA HCRs to generate elongated product (Figures 3b, d). Agarose gel analysis of reaction products confirmed highly orthogonal reactions and activation by SNA. LT-Input reacted with only L-*a*TNA hairpins, generating long chain product (Figure 4, lanes 3, 6), whereas DT-Input elongated D-*a*TNA hairpins (Figure 4, lane 4, 7). Addition of S-Input initiated elongation reactions in both D- and L-*a*TNA HCR (Figure 4, lanes 5, 8). These results clearly show that SNA can serve as interface that can connect between right-handed and left-handed nucleic acid circuits.

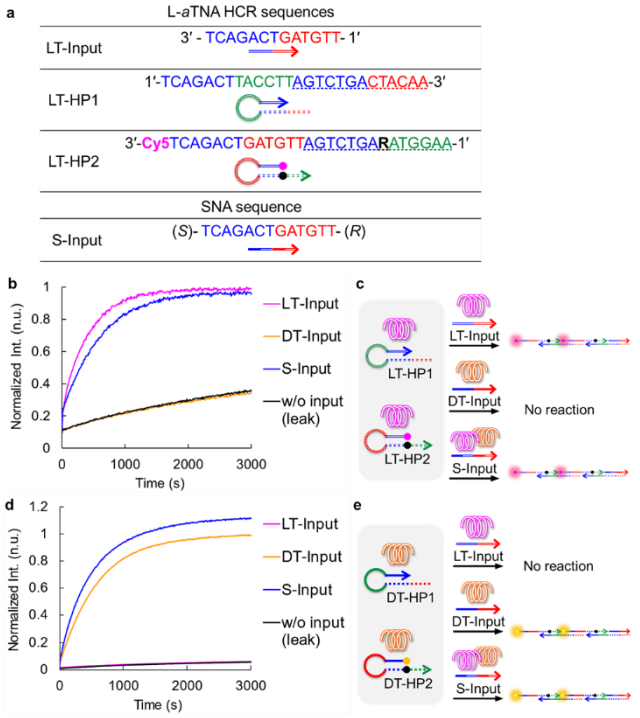

Figure 3. (a) Sequences used for L-*a*TNA HCR circuit with SNA input. (b) Time trace of emission intensity from L-*a*TNA HCR (c) Schematic illustration of orthogonal activation of L-*a*TNA HCR. (d) Time trace of emission intensity from D-*a*TNA HCR. (e) Schematic illustration of orthogonal activation of D-*a*TNA HCR. Conditions: 37 °C, 10 mM phosphate buffer, 200 mM NaCl, pH 7.0, 100 nM each hairpin, 20 nM (0.2 eq) input strand. Fluorescence intensity was normalized by the maximum emission after saturation of the reaction in the presence of corresponding input strand.

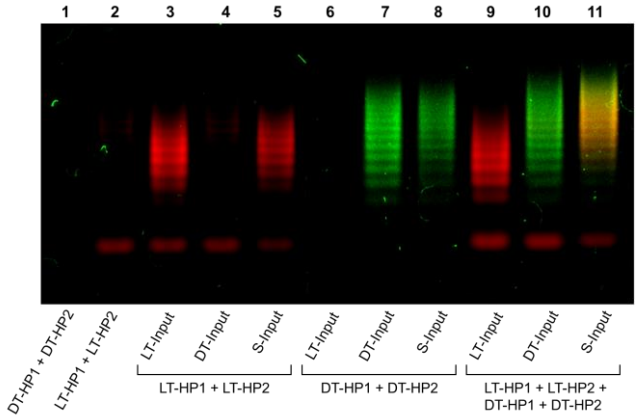

Figure 4. Agarose gel analysis (3 w/v%) of HCR product after 1 h incubation at 37 °C. Lane 1, D-*a*TNA hairpins without input; Lane 2, L-*a*TNA hairpins without input; Lanes 3-5, L-*a*TNA hairpins with indicated input; Lanes 6-8, D-*a*TNA hairpins with indicated input; Lanes 9-11, both D- and L-*a*TNA hairpins with indicated input.

Dual OR Logic Gate. To further demonstrate the utility of the orthogonality between two chiral *a*TNA HCRs, we designed and tested a dual OR gate system, which had D- and L-*a*TNA circuits in one solution (Figure 5a). Each input strand was added to the solution containing DT-H1, DT-H2, LT-H1, and LT-H2. As in experiments with only a D- or an L-*a*TNA HCR, in the solution with both *a*TNA hairpins, the HCRs were orthogonally activated by the addition of corresponding input strands, giving kinetics similar to those observed for single HCRs: LT-Input and DT-Input amplified Cy5 signal and Cy3 signal, respectively (Figure 5b, c). This result clearly indicated that there are no interactions between L-*a*TNA and D-*a*TNA even though the strand sequences are the same. This discrimination was achieved due to the helical preferences.

In the solution with both *a*TNA hairpins, the S-Input induced both signals because the SNA activated both L- and D-*a*TNA HCR (Figure 5d). Amplification kinetics in the presence of S-Input were slower than in the presence of LT-Input and DT-Input strands. We hypothesize that this was due to the competition between HCR circuits, which decreased the effective concentration of initiator for each HCR. Note that total concentration of the circuits (DT-HP plus LT-HP) was doubled in experiments with both *a*TNA hairpins (Figure 5) with respect to experiments with individual circuits (Figures 2 and 3), whereas the concentration of S-Input was the same. Product characterized using agarose gel electrophoresis was consistent with the kinetics (Figure 4, lane 9-11). These results confirm the remarkably high orthogonality between L-*a*TNA and D-*a*TNA in the HCR circuits and demonstrate that SNA communicates with both L- and D-*a*TNA. This system can be described as dual OR gate circuits that output two signals responding to input XNAs (Figure 5e).

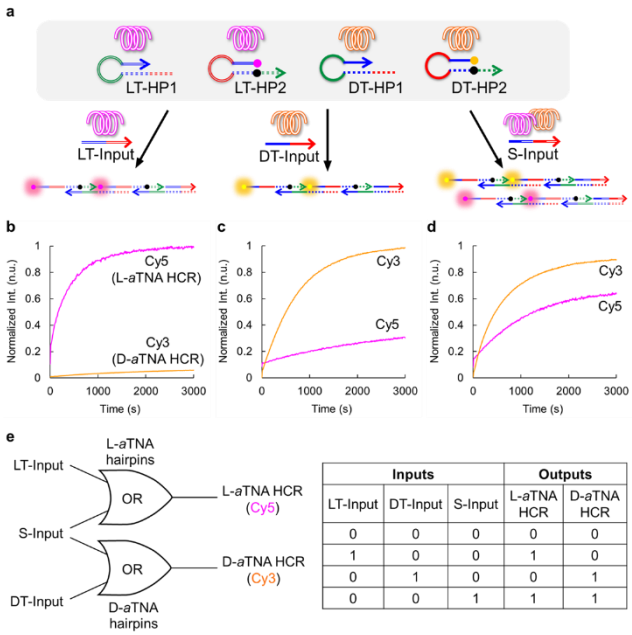

Figure 5. (a) Schematic illustration of orthogonal activation of *a*TNA HCR circuits. (b-d) Kinetics of mixed D- and L-*a*TNA HCR circuits triggered by (b) LT-Input, (c) DT-Input, and (d) S-Input. Conditions: 37 °C, 10 mM phosphate buffer, 200 mM NaCl, pH 7.0, 100 nM each hairpin, 20 nM input. (e) Schematic of design of dual OR logic gate and truth table.

RNA detection via SNA-mediated D-*a*TNA HCR. Finally, we designed an RNA-dependent signal amplification system with a D-*a*TNA HCR that is activated in the presence of target RNA through an SNA interface. A 23-mer RNA was used as model target. Due to the helicity mismatch, right-handed D-

RNA and left-handed D-*a*TNA are orthogonal unless an SNA is used to mediate recognition of sequence information. The SNA interface strands used in our experiment were designed to have a region complementary to the target RNA and another region that acts as the input to the D-*a*TNA HCR (Figure 6a). The SNA interface was designed to form a stem-loop structure that involves the region complementary to DT-H2 toehold when the target RNA is not present. The target RNA binds to loop and stem in (*S*)-termini of SNA interface strand, releasing the input region, resulting in activation of the D-*a*TNA circuit (Figure 6a). The T_m values of the S-I0s stem and of the S-I0s/RNA duplex were 59.6 ºC and 65.8 ºC, respectively (Figure S6) so these structures are stable under the conditions of circuit operation.

The reaction was performed by addition of DT-HP1 and DT-HP2 into the pre-annealed mixture of 0.2 eq. of S-10s and 0.2 eq. of target RNA. Importantly, the S-I0s strand without target RNA did not cause a leak reaction, whereas the target RNA induced the amplification of fluorescent signal (Figure 6b, blue lines). This reaction required use of high salt concentration (i.e., 1 M NaCl) for acceptably fast response, and only 30% emission was observed after 3000 s.

We reasoned that the low yield of this circuit resulted from propagation of helicity. We previously reported that the helicity of SNA can be induced by hybridization with helical nucleic acids composed of chiral scaffold.[52] In the RNA/SNA-interface complex, the propagation of right-handed helicity from RNA/SNA duplex into overhang input region reduced the rate of binding to the left-handed D-*a*TNA HCR. Such a helical propagation has also been reported in PNA/D-DNA/L-DNA system by Kundu et al.; in this case, right-handed helical propagation from the D-DNA/PNA duplex into single stranded region of the PNA significantly inhibited the binding to left-handed L-DNA.[53] Thus, the helical mismatch between the initiator complex and the D-*a*TNA hairpin likely led to the slow reaction.

The helicity propagation in SNA is guided by the base stacking.[52] We therefore hypothesized that use of a spacer could inhibit the helical propagation. To test this, one, two, or three C3 spacers were incorporated between RNA binding region and input region in SNA-interface (Figure 6a, S-I1s, S-I2s, and S-I3s, respectively). The T_m values were not so affected by incorporation of the spacer (Figure 4S). Analyses of fluorescence emission in the presence of these interfaces indicated that the C3 spacer significantly accelerated the signal amplification of D-*a*TNA HCR (Figure 6b). The more spacers incorporated in the SNA interface, the faster signal amplification. With the S-I2s interface, the fluorescent signals were approximately 80% at 3000 s. Importantly, incorporation of the C3 spacer did not cause significant leakage as similar kinetics were observed for S-I0s, S-I1s, and S-I2s in the absence of target, although the S-I3s interface slightly amplified the leakage. Thus, with S-I2s, orthogonal detection of a target RNA via a D-*a*TNA HCR circuit was achieved with fast reaction rate, sufficient reaction efficiency, and low leak. The amplification rate of this system depended on the concentration of the target (Figure S7), showing detection of 500 pM target RNA with distinct enhancement of fluorescent emission. Note that the initiation of HCR was also confirmed only by the addition of target RNA without pre-annealing process (Figure S8). To prove the possibility of in vivo using, we evaluated SNA-mediated D-*a*TNA HCR circuit targeting RNA in 10% FBS (Figure S9). Sufficiently high nuclease resistance of D-*a*TNA and SNA enabled correct activation of signal amplification only in the presence of target RNA, clearly indicating the potential of this XNA-HCR system for RNA detection in vivo.

HCR circuits have rarely been exploited *in vivo* due to nonspecific interactions between the circuit and contaminating DNA and RNA and degradation by nucleases, which result in false positive signals. These problems are resolved by the D-*a*TNA HCR/SNA interface system. As HCR elongation occurs on the target RNA, this suggests that target can be localized using this system.

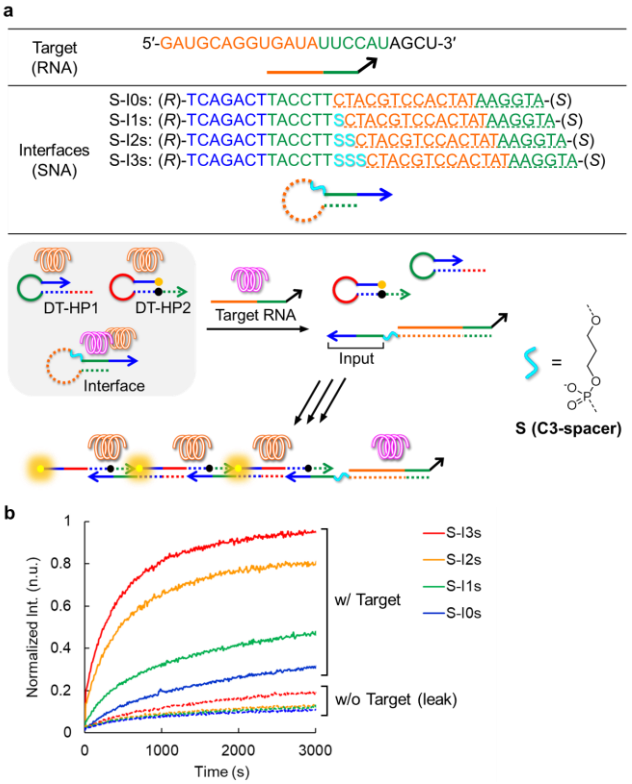

Figure 6. (a) Sequence design and schematic illustration of RNA detection using D-*a*TNA HCR mediated by an SNA interface. (b) Kinetics of D-*a*TNA HCR triggered by of the indicated SNA interface and target RNA. Conditions: 37 ºC, 10 mM phosphate buffer, 1.0 M NaCl, pH 7.0, 100 nM each hairpin, 20 nM indicated SNA interface, and 20 nM target RNA.

CONCLUSIONS

We have developed an HCR circuit composed of *a*TNA. The extremely high thermal stability of *a*TNA duplexes enabled design of an HCR circuit with short oligomers, resulting in a rapid elongation reaction and minimal leakage. Enzymatic durability was also confirmed. D-*a*TNA HCR and L-*a*TNA HCR worked as an orthogonal system due to the opposite helicities of these two XNAs. An SNA input activated both *a*TNA HCRs. When both were present in solution, D-*a*TNA and L-*a*TNA HCRs were correctly activated in response to corresponding D-*a*TNA or L-*a*TNA input strands without interference, resulting in a dual OR gate circuit. An SNA with appropriate spacer enabled an orthogonal D-*a*TNA HCR circuit to be triggered by D-RNA. This strategy will be applicable to other heterochiral nucleic acid circuits. Due to high nuclease resistance, sufficient solubility, and highly orthogonal detection the SNA-mediated D-aTNA HCR hold promises for reliable visualization and localization of target RNA in cell and biopsy.

ASSOCIATED CONTENT

Supporting Information.
This material is available free of charge via the Internet at http://pubs.acs.org."
Additional experimental materials, methods, chemical structures of dyes, melting profiles of HPs, long-time reaction of D-*a*TNA HCR, gel analysis with DNA ladder, nuclease durability, melting profiles of SNA interface, effect of target concentration, reaction without annealing, robustness of SNA-mediated D-*a*TNA HCR circuits, and MS data for all sequences.

AUTHOR INFORMATION

Corresponding Author

*E-mail: murayama@chembio.nagoya-u.ac.jp, asanuma@chembio.nagoya-u.ac.jp.

ORCID

Keiji Murayama: 0000-0002-6537-0120
Hiroyuki Asanuma: 0000-0001-9903-7847

Notes

The authors declare no competing financial interest.

ACKNOWLEDGMENT

This work was supported by Grant-in-Aid for Transformative Research Areas "Molecular Cybernetics" JP20H05970 (K.M.) and JSPS KAKENHI grants JP20K15399 (K.M.) and JP21H05025 (H.A.). AMED under Grant Number 21am0401007 (H.A.) is also acknowledged.

REFERENCES

(1) Simmel, F. C.; Yurke, B.; Singh, H. R. Principles and Applications of Nucleic Acid Strand Displacement Reactions. *Chem. Rev.* **2019**, *119*, 6326–6369.
(2) Seelig, G.; Soloveichik, D.; Zhang D. Y.; Winfree, E. Enzyme-free nucleic acid logic circuits. *Science* **2006**, *314*, 1585–1588.
(3) Sakamoto, K.; Gouzu, H.; Komiya K.; Kiga, D.; Yokoyama, S.; Yokomori, T.; Hagiya, M. Molecular Computation by DNA Hairpin Formation. *Science* **2010**, 288, 1223–1226.
(4) Yordanov, B.; Kim, J.; Petersen, R. L.; Shundy, A.; Kulkarni, V. V.; Phillips, A. Computational Design of Nucleic Acid Feedback Control Circuits. *ACS Synth. Biol.* **2014**, *3*, 600–616.
(5) Watson, E. E.; Angerani, S.; Sabale, P. M.; Winssinger, N. Bio-supramolecular Systems: Integrating Cues into Responses. *J. Am. Chem. Soc.* **2021**, *143*, 4467–4482.
(6) Dirks, R. M.; Pierce, N. A. Triggered Amplification by Hybridization Chain Reaction. *Proc. Natl. Acad. Sci. U. S. A.* **2004**, *101*, 15275–15278.
(7) Zhang, D. Y.; Chen, S. X.; Yin, P. Optimizing the specificity of nucleic acid hybridization. *Nat. Chem.* **2012**, *4*, 208−214.
(8) Xuan, F.; Hsing, I.-M. Triggering hairpin-free chain-branching growth of fluorescent DNA dendrimers for nonlinear hybridization chain reaction. *J. Am. Chem. Soc.* **2014**, *136*, 9810−9813.
(9) Angerani, S.; Winssinger, N.; Sense-and-Release Logic-Gated Molecular Network Responding to Dimeric Cell Surface Proteins. *J. Am. Chem. Soc.* **2020**, *142*, 12333–12340.
(10) Yurke, B.; Turberfield, A. J.; Mills Jr, A. P.; Simmel, F. C.; Neumann, J. L. A DNA-fuelled molecular machine made of DNA. *Nature* **2000**, *406*, 605–608.
(11) Wang, F.; Lu, C.-H.; Willner, I. From Cascaded Catalytic Nucleic Acids to Enzyme–DNA Nanostructures: Controlling Reactivity, Sensing, Logic Operations, and Assembly of Complex Structures. *Chem. Rev.* **2014**, *114*, 2881–2941.
(12) Tomov, T. E.; Tsukanov, R.; Glick, Y.; Berger, Y.; Liber, M.; Avrahami, D.; Gerber, D.; Nir, E. DNA bipedal motor achieves a large number of steps due to operation using microfluidics-based interface. *ACS Nano* **2017**, *11*, 4002−4008.
(13) Sato, Y.; Hiratsuka, Y.; Kawamata, I.; Murata, S.; Nomura, S. M. Micrometer-sized molecular robot changes its shape in response to signal molecules. *Sci. Robot.* **2017**, *2*, eaal3735.
(14) Meng, W.; Muscat, R. A.; McKee, M. L.; Milnes, P. J.; El-Sagheer, A. H.; Bath, J.; Davis, B. G.; Brown, T.; O'Reilly, R. K.; Turberfield, A. J. An Autonomous Molecular Assembler for Programmable Chemical Synthesis. *Nat. Chem.* **2016**, *8*, 542–548.
(15) Zhang, Y.; McMullen, A.; Pontani, L.-L.; He, X.; Sha, R.; Seeman, N. C.; Brujic, J.; Chaikin, P. M. Sequential self-assembly of DNA functionalized droplets. *Nat. Commun.* **2017**, *8*, 21.
(16) McMillan, J. R.; Hayes, O. G.; Remis, J. P.; Mirkin, C. A. Programming Protein Polymerization with DNA. *J. Am. Chem. Soc.* **2018**, *140*, 15950–15956.
(17) Cangialosi, A.; Yoon, C.; Liu, J.; Huang, Q.; Guo, J.; Nguyen, T. D.; Gracias, D. H.; Schulman, R. DNA sequence-directed shape change of photopatterned hydrogels via high-degree swelling. *Science* **2017**, *357*, 1126−1130.
(18) Kahn, J. S.; Hu, Y.; Willner, I. Stimuli-Responsive DNA-Based Hydrogels: From Basic Principles to Applications. *Acc. Chem. Res.* **2017**, *50*, 680–690.
(19) Leumann, C. J. DNA Analogues: From Supramolecular Principles to Biological Properties. *Bioorg. Med. Chem.* **2002**, *10*, 841-854.
(20) Petersen, M.; Wengel, J. LNA: a versatile tool for therapeutics and genomics. *Trends Biotechnol.* **2003**, *21*, 74–81.
(21) Pinheiro, V. B.; Holliger, P. The XNA world: progress towards replication and evolution of synthetic genetic polymers. *Curr. Opin. Chem. Biol.* **2012**, *16*, 245-252.
(22) Chaput, J. C.; Herdewijn, P. What Is XNA? *Angew. Chem. Int. Ed.* **2019**, *58*, 11570-11572.
(23) Murayama, K.; Asanuma, H. Design and Hybridization Properties of Acyclic Xeno Nucleic Acid Oligomers. *ChemBioChem*, **2021**, *22*, 2507-2515.
(24) Zhang, L.; Peritz, A.; Meggers, E. A Simple Glycol Nucleic Acid. *J. Am. Chem. Soc.* **2005**, *127*, 4174–4175.
(25) Egli, M.; Pallan, P. S.; Pattanayek, R.; Wilds, C. J.; Lubini, P.; Minasov, G.; Dobler, M.; Leumann, C. J.; Eschenmoser, A. Crystal Structure of Homo-DNA and Nature's Choice of Pentose over Hexose in the Genetic System. *J. Am. Chem. Soc.* **2006**, *128*, 10847–10856.
(26) Ueno, Y.; Kawamura, A.; Takasu, K.; Komatsuzaki, S.; Kato, T.; Kuboe, S.; Kitamura, Y.; Kitade, Y. Synthesis and Properties of a Novel Molecular Beacon Containing a Benzene-Phosphate Backbone at Its Stem Moiety. *Org. Biomol. Chem.* **2009**, *7*, 2761–2769.
(27) Asanuma, H.; Toda, T.; Murayama, K.; Liang, X.G.; Kashida, H. Unexpectedly stable artificial duplex from flexible acyclic threoninol. *J. Am. Chem. Soc.*, **2010**, *132*, 14702-14703.
(28) Srivastava, P.; Abou El Asrar, R.; Knies, C.; Abramov, M.; Froeyen, M.; Rozenski, J.; Rosemeyer, H.; Herdewijn, P. Achiral, Acyclic Nucleic Acids: Synthesis and Biophysical Studies of a Possible Prebiotic Polymer. *Org. Biomol. Chem.* **2015**, *13*, 9249–9260.
(29) Beck, K. M.; Sharma, P. K.; Hornum, M.; Risgaard, N. A.; Nielsen, P. Double-headed nucleic acids condense the molecular information of DNA to half the number of nucleotides. *Chem. Commun.* **2021**, *57*, 9128-9131.
(30) Young, B. E.; Kundu, N.; Sczepanski, J. T. Mirror-Image Oligonucleotides: History and Emerging Applications. *Chem. Eur. J.* **2019**, *25*, 7981–7990.
(31) Klußmann, S.; Nolte, A.; Bald, R.; Erdmann, V. A.; Fürste, J. P. Mirror-Image RNA That Binds D-Adenosine. *Nat. Biotechnol.* **1996**, *14*, 1112–1115.
(32) Sczepanski, J. T.; Joyce, G. F. Binding of a Structured D-RNA Molecule by an L-RNA Aptamer. *J. Am. Chem. Soc.* **2013**, *135*, 13290–13293.
(33) Feagin, T. A.; Olsen, D. P. V.; Headman, Z. C.; Heemstra, J. M. High-Throughput Enantiopurity Analysis Using Enantiomeric DNA-Based Sensors. *J. Am. Chem. Soc.* **2015**, *137*, 4198–4206.
(34) Ke, G.; Wang, C.; Ge, Y.; Zheng, N.; Zhu, Z.; Yang, C. J. L-DNA Molecular Beacon: A Safe, Stable, and Accurate Intracellular Nano-Thermometer for Temperature Sensing in Living Cells. *J. Am. Chem. Soc.* **2012**, *134*, 18908–18911.

(35) Kim, Y.; Yang, C. J.; Tan, W. Superior Structure Stability and Selectivity of Hairpin Nucleic Acid Probes with an L-DNA Stem. *Nucleic Acids Res.* **2007**, *35*, 7279–7287.
(36) Kabza, A. M.; Young, B. E.; Sczepanski, J. T. Heterochiral DNA Strand-Displacement Circuits. *J. Am. Chem. Soc.* **2017**, *139*, 17715–17718.
(37) Sacui, I.; Hsieh, W. C.; Manna, A.; Sahu, B.; Ly, D. H. Gamma Peptide Nucleic Acids: As Orthogonal Nucleic Acid Recognition Codes for Organizing Molecular Self-Assembly. *J. Am. Chem. Soc.* **2015**, *137*, 8603–8610.
(38) Hsieh, W. C.; Martinez, G. R.; Wang, A.; Wu, S. F.; Chamdia, R.; Ly, D. H. Stereochemical Conversion of Nucleic Acid Circuits via Strand Displacement. *Commun. Chem.* **2018**, *1*, 89.
(39) Chang, D.; Lindberg, E.; Winssinger, N. Critical Analysis of Rate Constants and Turnover Frequency in Nucleic Acid-Templated Reactions: Reaching Terminal Velocity. *J. Am. Chem. Soc*. **2017**, *139*, 1444–1447.
(40) Kashida, H.; Murayama, K.; Toda, T.; Asanuma, H. Control of the Chirality and Helicity of Oligomers of Serinol Nucleic Acid (SNA) by Sequence Design. *Angew. Chem. Int. Ed.* **2011**, *50*, 1285–1288.
(41) Murayama, K.; Kashida, H.; Asanuma, H. Acyclic L-Threoninol Nucleic Acid (L-*a*TNA) with Suitable Structural Rigidity Cross-pairs with DNA and RNA. *Chem. Commun.* **2015**, *51*, 6500-6503.
(42) Murayama, K.; Nagao, R.; Asanuma, H. D-*a*TNA Circuit Orthogonal to DNA Can Be Operated by RNA Input via SNA. *ChemistrySelect* **2017**, *2*, 5624–5627.
(43) Choi, H. M. T.; Chang, J. Y.; Trinh, L. A.; Padilla, J. E.; Fraser, S. E.; Pierce, N. A. Programmable in situ amplification for multiplexed imaging of mRNA expression. *Nat. Biotechnol.* **2010**, *28*, 1208−1214.
(44) Zhu, G.; Zheng, J.; Song, E.; Donovan, M.; Zhang, K.; Liu, C.; Tan, W. Self-Assembled, Aptamer-Tethered DNA Nanotrains for Targeted Transport of Molecular Drugs in Cancer Theranostics. *Proc. Natl. Acad. Sci. U. S. A.* **2013**, *110*, 7998– 8003.
(45) Chatterjee, G.; Dalchau, N.; Muscat, R. A.; Phillips, A.; Seelig, G. A spatially localized architecture for fast and modular DNA computing. *Nat. Nanotechnol.* **2017**, *12*, 920−927.
(46) Bi, S.; Yue, S.; Zhang, S. Hybridization chain reaction: a versatile molecular tool for biosensing, bioimaging, and biomedicine. *Chem. Soc. Rev.* **2017**, *46*, 4281−4298.
(47) Prinzen, A. L.; Saliba, D.; Hennecker, C.; Trinh, T.; Mittermaier, A.; Sleiman, H. F. Amplified Self-Immolative Release of Small Molecules by Spatial Isolation of Reactive Groups on DNA-Minimal Architectures. *Angew. Chem., Int. Ed.* **2020**, *59*, 12900–12908.
(48) Morihiro, K.; Moriyama, Y.; Nemoto, Y.; Osumi, H.; Okamoto, A. anti–syn Unnatural Base Pair Enables Alphabet-Expanded DNA Self-Assembly. *J. Am. Chem. Soc.* **2021**, *143*, 14207–14217.
(49) Kim, K. T.; Angerani, S.; Chang, D.; Winssinger, N. Coupling of DNA Circuit and Templated Reactions for Quadratic Amplification and Release of Functional Molecules. *J. Am. Chem. Soc.* **2019**, *141*, 16288–16295.
(50) Ang, Y. S.; Yung, L. Y. L. Rational Design of Hybridization Chain Reaction Monomers for Robust Signal Amplification. *Chem. Commun.* **2016**, *52*, 4219–4222.
(51) Kim, K. T.; Angerani, S.; Winssinger, N. A minimal hybridization chain reaction (HCR) system using peptide nucleic acids. *Chem. Sci.*, **2021**, *12*, 8218–8223.
(52) Kashida, H.; Nishikawa, K.; Shi, W.; Miyagawa, T.; Yamashita, H.; Abe, M.; Asanuma, H. A Helical Amplification System Composed of Artificial Nucleic Acids. *Chem. Sci.* **2021**, 12, 1656–1660.
(53) Kundu, N.; Young, B. E.; Sczepanski, J. T. Kinetics of Heterochiral Strand Displacement from PNA-DNA Heteroduplexes. *Nucleic Acids Res.* **2021**, *49*, 6114–6127.

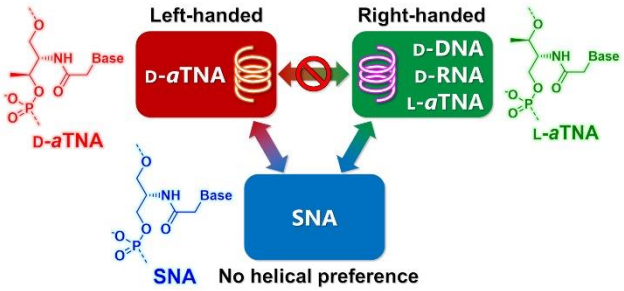
Left-handed
Right-handed
D-aTNA
D-DNA
D-RNA
L-aTNA
NH
Base
D-aTNA
L-aTNA
SNA
SNA
No helical preference